

RESEARCH

Open Access



Key mechanism of enzymatic dehairing technology for leather-making: permeation behaviors of protease into animal hide and the mechanism of charge regulation

Mengchu Gao^{1,2}, Jinzhi Song^{1,2}, Xu Zhang^{1,2}, Chunxiao Zhang^{1,2}, Biyu Peng^{1,2*}  and Sadaqat Ali Chattha^{1,3}

Abstract

Enzymes have been widely used as alternatives to conventional chemicals in cleaner leather processes due to their advantages of meeting increasing environmental demands. Especially, enzymatic unhairing based on protease has been applied to leather-making for a long time, however, it still has the key problem of slow permeation in the animal hide, resulting in slow unhairing rate, poor hair removal effect, excessive proteolysis of hide collagen, and decreased leather quality. Aiming at the key problem of bio-unhairing technology, fluorescent labeling technique and confocal laser scanning microscopy were used to investigate the protease permeation behaviors into the animal hide based on well-prepared labeled proteases, as well as the quantitative analysis of the protease amount in different hide layers. The results show that the protease mainly permeates the bovine hide through transfollicular routes from the hair side, and although the intercellular-interfibrillar pathway also exists, it does not play an important role. Additionally, the protease permeation behaviors into the hide are greatly impacted by the charge states of the hide and protease proteins, depending on the isoelectric points (pI) of the proteins and solution pH values. When the solution pH is not between the pI values of the two proteins, the similarly charged protease can quickly and deeply penetrate the hide because of the electrostatic repulsion. The established mechanism provides a theoretical basis for developing an efficient enzymatic unhairing technology for leather-making, and this can also be applied to other processes involving the enzyme permeation into the hide or leather.

Keywords Protease, Permeation, Hair follicle, Enzymatic dehairing

*Correspondence:

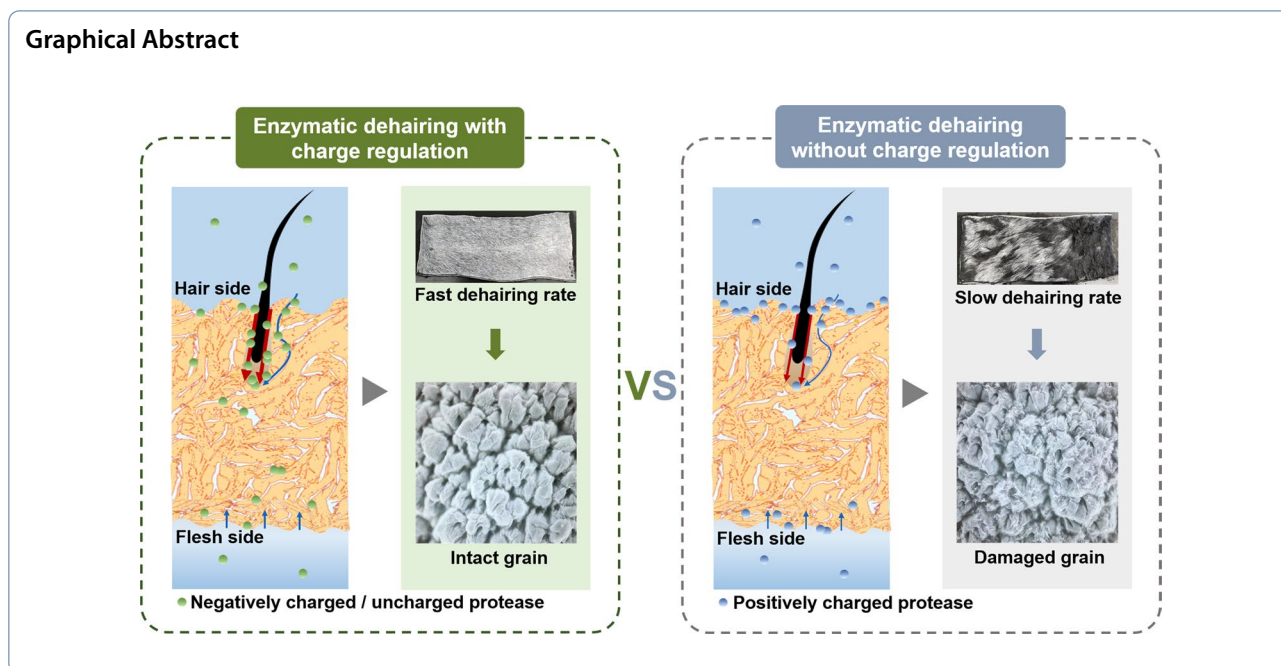
Biyu Peng

pengbiyu@scu.edu.cn

Full list of author information is available at the end of the article



© The Author(s) 2023. **Open Access** This article is licensed under a Creative Commons Attribution 4.0 International License, which permits use, sharing, adaptation, distribution and reproduction in any medium or format, as long as you give appropriate credit to the original author(s) and the source, provide a link to the Creative Commons licence, and indicate if changes were made. The images or other third party material in this article are included in the article's Creative Commons licence, unless indicated otherwise in a credit line to the material. If material is not included in the article's Creative Commons licence and your intended use is not permitted by statutory regulation or exceeds the permitted use, you will need to obtain permission directly from the copyright holder. To view a copy of this licence, visit <http://creativecommons.org/licenses/by/4.0/>.



1 Introduction

Instead of using sulphides to remove the hair from the animal hide in the traditional hair removal process, enzymatic dehairing utilizes enzymes, especially proteases, to remove the hair with several environmental benefits, such as reducing the quantity of solid sludge containing sulfates, the content of biochemical oxygen demand (BOD), and the content of chemical oxygen demand (COD) in the effluent[1–4]. There are some hypotheses as to the mechanism of enzymatic dehairing. A widely believed mechanism is that the enzyme action on the soft keratin in the hair bag and hair root sheath impairs the connection between the hair papilla and hair bulb to make the hair root loosen[5]. Since the hair bulb holding the hair papilla primarily consists of non-structural proteins, it can be an attack site in the process of protease-mediated dehairing[6]. The proteases without collagen hydrolytic activity are well appreciated by most researchers, which can weaken hide collagen damage to a great extent[7–10]. However, it takes a long time for a protease to reach the site between the hair bulb and hair papilla in the dehairing process. A study performed by Yates concluded that approximately 70% of the dehairing time was accounted for the enzyme diffusion to the hair follicle bottom[11]. Therefore, the hide collagen, especially the grain collagen on the superficial hide layer, tends to be excessively hydrolyzed, resulting in an ultimately negative effect on leather quality.

An effective way of weakening the excessive collagen proteolysis of grain would be to increase the protease

permeation rate, and various attempts have been made to achieve this goal. The protease permeation speed into the animal hide is influenced by its concentration. In response to an increase in the protease dosage, the process of protease permeation into the animal hide will be mostly sped up. But the grain damage may become severe with the increasing protease dosage because of the protease overload in the grain layer. It has been reported that the enzyme with a low molecular weight tends to have a faster penetration rate in the animal hide, avoiding the excessive action caused by the enzyme staying on the hide surface for a long time[12, 13]. Some researchers believe that firstly using glycosidases to destroy the proteoglycans in the interfibrillar substance, and then using proteases for hair removal can reduce the protease amount and processing time, decrease the degree of enzyme action on the hide collagen, especially the grain collagen[14]. And some strategies use sulfhydryl compounds or neutral proteases to remove the epidermis before enzymatic dehairing, which can weaken the permeation barrier for the dehairing protease[15]. The application of surfactants may improve the protease permeation speed from the reduction of interfacial tension and the change in surface charge on the protease[16]. Additionally, temperature, pH, and mechanical force also affect protease permeation. It's worth noting that the pH can affect not only the protease activity but also its surface charge, thus impacting its permeation behaviors into the hide. The surface charges are associated with the ionizable

residues on the surfaces of protease and skin, resulting in electrostatic interactions[17]. The type of charge that produces a better permeation effect remains a source of debate among researchers. Some researchers believe that the opposite charges of substance and skin are more conducive to substance penetration, while others hold the belief that the same charges or without charges would achieve a good permeation effect of substance[18–30].

It is speculated that the majority of molecules penetrate the animal hide via intercellular-interfibrillar routes,

transcellular-interfibrillar routes, and transappendageal (transfollicular) routes (Fig. 1a) [31]. It has been concluded that it is difficult for a substance with a molecular weight greater than 500 Da to pass through the stratum corneum[32]. Because of the large size of the enzyme molecule and the inviable cells of raw animal hide used for leather processing, it is unlikely that the protease penetrates the hide through transcellular-interfibrillar routes. However, in the dehairing method of enzymatic painting, the enzyme diffuses through the flesh layer when applied to the flesh surface. And even the enzyme

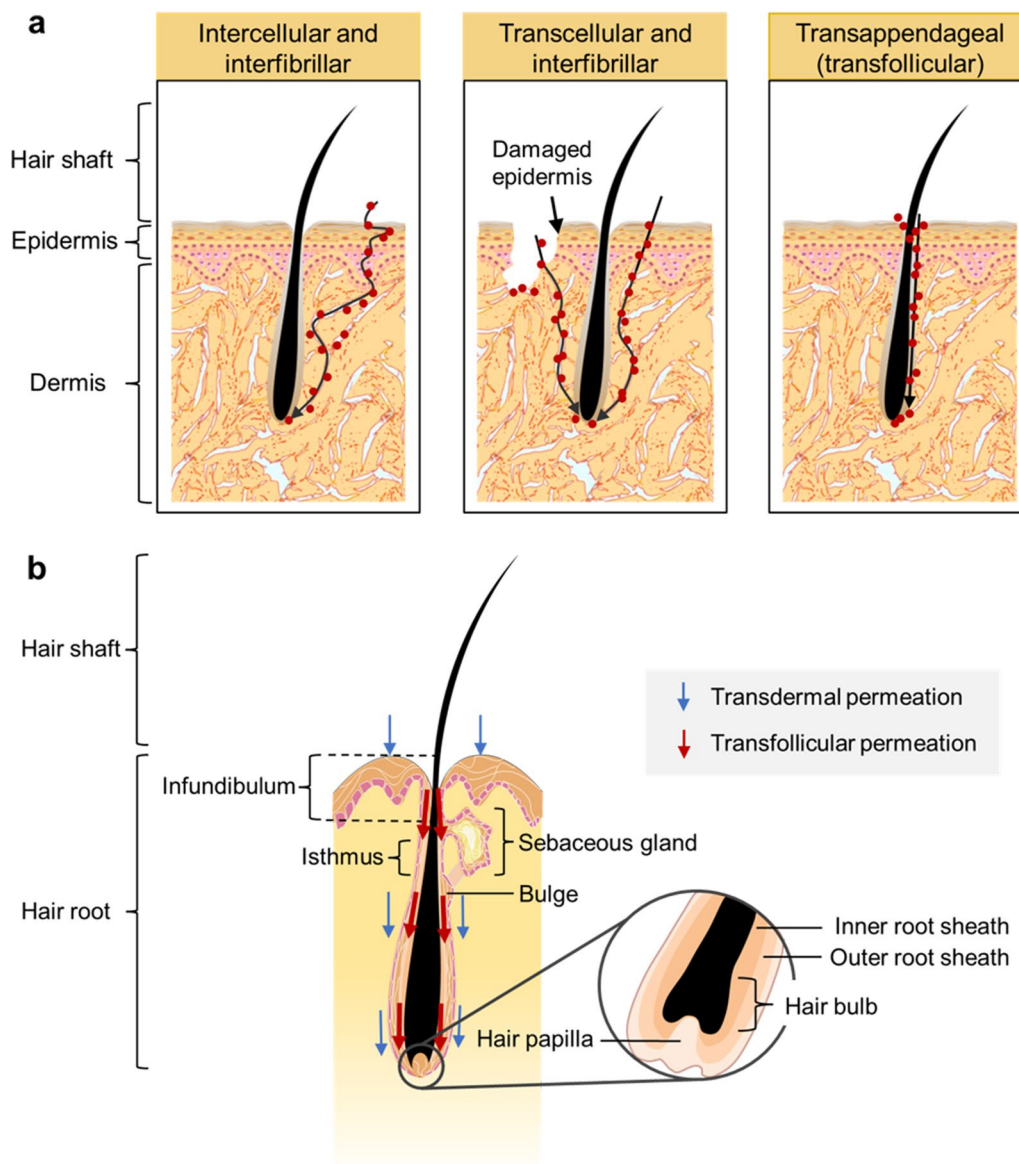


Fig. 1 Schematic illustration of possible permeation routes and types of enzymes in the animal hide during the enzymatic dehairing process. **a** Schematic diagram of possible permeation routes of enzyme molecules in the animal hide. **b** Schematic of hair follicle structure and enzyme permeation types during the enzymatic dehairing process

is subjected to contact with both hide sides, there is a faster diffusion rate of the applied enzyme through the flesh side rather than through the hair surface[33]. Therefore, the intercellular-interfibrillar route exists during the protease penetration into the animal hide. Transfollicular pathways have long been believed to play a limited role in protease permeation due to their small proportion of animal hide appendages compared to the whole hide[34]. The hair follicle is an appendage of animal hide, made up of a superficial portion and an inferior structure consisting of the hair bulb. The superficial area of the hair follicle can be further divided into the hair infundibulum and isthmus (Fig. 1b). The hair follicular opening surface is keratinized, whereas corneocytes in the deeper hair infundibulum are smaller and crumblier, suggesting an incomplete hide barrier[35]. However, Lauer holds that the keratinous layers of inner and outer root sheaths might physically prevent molecules from contacting the hair bulb[36]. Even so, the invaginations of hair follicles extend deeply into the dermis, significantly increasing the surface area available for substance permeation. Therefore, the transfollicular route appears to be a possible permeation pathway.

The protease permeation behaviors into the animal hide are expected to be detectable. As an acceptable and visual method, the fluorescent labeling technique is available. A kind of fluorescein is covalently bound with the enzyme molecule to give the labeled protein fluorescence characteristics. Thus, the localization and trace of fluorescently labeled proteins in cells or tissues can be realized, and the results are sensitive and intuitive. However, compared with the unlabeled protease, the fluorescently labeled protease may vary in the molecule weight, isoelectric point (pI), enzyme activity, and other aspects, therefore, these properties influencing protease penetration behaviors need to be investigated before permeation experiments. Subsequently, confocal laser scanning microscopy (CLSM) can be collocated with the fluorescent labeling technique to image the permeation route and extent of fluorescently labeled proteases in the hide. In terms of technical advantages, CLSM is characterized by its high resolution, high definition, and visualization of multiple depths without mechanical sectioning[37]. Up to now, some researchers have utilized the fluorescent labeling technique to investigate the permeation process of protease into animal hide in leather processing, but most of the studies focused on the permeation depth of fluorescently labeled enzymes and their contents in hide layers qualitatively represented by fluorescence intensities [38]. In general, these studies did not address the change in enzyme properties after fluorescent labeling in enough detail, and could not ensure that the

permeation behaviors of prepared fluorescently labeled enzymes in the animal hide were consistent with that of the original enzymes. Thus, it's still unclear how the enzyme penetrates the animal hide during enzymatic leather processing.

As mentioned above, it is necessary to investigate the process and law of protease permeation behaviors in the animal hide, thus guiding the enzyme selection and enzymatic process regulation in leather-making. Herein, the objective of this work is to investigate the permeation behaviors of proteases in the hide with the techniques of fluorescent labeling and CLSM, involving tracking the protease permeation routes in the animal hide, determining their permeation directions, and comparing their permeation depths and rates at varying pH conditions. Furthermore, quantitatively analyzing the permeation process of proteases from the hair side is carried out to confirm the permeation experiment results of fluorescently labeled proteases, and the charge regulation mechanism of protease permeation behaviors into the animal hide is established.

2 Materials and methods

2.1 Materials

Alkaline protease P-SG-B and P-U-B were provided by Sichuan Dowell Technology Co., Ltd. (Chengdu, China); neutral protease P-LKT-N was provided by Shandong Lonct Enzymes Co., Ltd. (Linyi, China). Analytical and industrial grade chemicals were used in biochemical analysis and leather processing, respectively.

2.2 Preparation and characterization of fluorescently labeled proteases

2.2.1 Preparation of fluorescently labeled proteases

Fluorescently labeled proteases, named FITC-P-U-B, FITC-P-LKT-N, and FITC-P-SG-B, were chemically synthesized as the modified method[39]. Each protease was dissolved in a mixture of saline solution and 0.5 mol/L carbonate buffer (pH 9.0) to contain 10 mg of protein per milliliter, and then an appropriate amount of FITC was added. The reaction mixture was kept at 0–4 °C and in the dark for 12–14 h while being stirred continuously at a slow speed. Subsequently, labeled proteins were precipitated with a half saturation ammonium sulfate solution to remove unbound fluorescein, followed by dialysis against an excess amount of cold (0–4 °C) 0.01 mol/L PBS buffer (pH 7.2) to remove ammonium sulfate. A Nessler's reagent was used to test until the dialyzed solution was free of ammonium ions. Before the following characterization and permeation experiments, fluorescently labeled proteases were temporarily stored in the dark at 4 °C.

2.2.2 UV-Vis and fluorescence spectrum measurements

As the samples were appropriately diluted with a certain volume of PBS buffer, a quartz cuvette with a path length of 1 cm was used for measuring these samples at wavelengths between 200 and 800 nm at a scanning rate of 2 nm/s and a resolution of 0.2 in a volume of 1.5 mL. It was conducted in the same volume of deionized water that was used for the baseline correction. Similarly, a fluorophotometer (F7000, Hitachi Ltd., Japan) was used to scan the fluorescence intensities of the three fluorescently labeled protease solutions with slits of 5 nm for both excitation and emission monochromators and an integration time of 0.1 s. The fluorescence spectra were determined at room temperature (25 °C) using a four-sided quartz cuvette with a path length of 1 cm. A step size of 2 nm had been implemented for the excitation wavelength range from 400 to 550 nm, and also a step size of 2 nm was carried out for the emission wavelength range from 505 to 600 nm.

2.2.3 Thin layer chromatography analysis

The FITC-labeled proteases with dialysis were analyzed by thin layer chromatography (TLC), and the FITC-labeled proteases without dialysis, as well as the FITC monomer, were also analyzed. A TLC silica gel plate was used as the carrier, and a small amount of sample was gently taken by a capillary to the thin layer silica gel plate, and then samples were spread out with an n-propanol aqueous solution (3:1, V/V). Chromatography was carried out for about 25–30 min, and the fluorescence signals were observed under 365 nm. Since subsequent permeation experiments would be performed at different pH values for a long time, it was necessary to assess the stability of fluorescently labeled proteases. The FITC-labeled protease solutions were incubated at varying pH values (6.5–10.5) for 5 h at 30 °C, which was consistent with the actual enzymatic dehairing conditions. Then TLC tests were also conducted to determine whether the fluorescein monomer was released after incubation.

2.2.4 Binding degree of fluorescein to protein determination

To determine the amount of bound fluorescein, a fluorescein quantitative standard curve was required. 1 mg of FITC was accurately weighed, dissolved in 10 mL of 0.5 mol/L carbonate buffer (pH 9.0), and then diluted to 100 mL with 0.01 mol/L PBS buffer (pH 7.2). The fluorescein solution of 10 µg/mL was used as the stock solution, and then diluted to different concentrations as required. Their absorbances were measured at 490 nm, and the absorbance was taken as the ordinate while the fluorescein content as the abscissa to make the standard curve. Subsequently, the bound fluorescein amount of each FITC-labeled protease was determined according

to the fluorescein quantitative standard curve, and Lowry's method was used to determine their protein contents[40]. The binding degree of fluorescein to protein was calculated as the detected fluorescein content (g) per gram of fluorescently labeled protein.

2.2.5 Electrophoresis analysis

The molecular weights of unlabeled proteases and FITC-labeled proteases were evaluated by 12% SDS-PAGE electrophoresis according to the Laemmli method[41], and their pI values were determined by isoelectric focusing (IEF) electrophoresis. The SDS-PAGE electrophoresis analysis was carried out with an electrophoresis cell (Mini-PROTEAN® Tetra, Bio-rad, American), and the IEF electrophoresis was conducted with a Mini IEF Cell (Model 111, Bio-rad, American). All the electrophoresis-related reagents were purchased from Bio-rad, and specific operations referred to the Bio-rad's electrophoresis protocol. The SDS-PAGE gel was firstly treated under 100 V for the sample to move to the dividing line between the stacking gel and separation gel, subsequently, the voltage was increased to 150 V and the electrophoresis continued until the sample reached the lower edge of the separation gel. The IEF gel was focused under constant voltages in a stepwise mode as follows: 100 V for 30 min, 200 V for 15 min, and 450 V for 60 min. Whereafter all the gels were fixed and stained by colloid Coomassie Brilliant Blue, and decolorized with deionized water. The molecular weights and pI values of proteases were calculated using Quantity One software (Bio-rad, American).

2.2.6 Proteolytic activity assay

The Folin-Ciocalteu method was used to determine the protease activity based on the casein substrate[42]. One casein hydrolytic activity unit of the protease represented the enzyme quantity that produced 1 µg of tyrosine in one minute. Similarly, the collagen hydrolytic activities of unlabeled proteases and FITC-labeled proteases were determined using native hide powder as the substrate, and the specific procedure referred to in our previous work[43]. One collagen hydrolytic activity unit was defined as the enzyme amount that generated 1 µg of hydroxyproline per minute. All measurements were carried out at 30 °C and various pH values.

2.3 Permeation experiments

For the permeation experiment, a full-thickness fleshed wet-salted bovine hide was used, which was thoroughly washed to remove salt, dirt, and blood. Afterward, a conventional soaking step was conducted, and the subcutaneous tissue was removed without damaging other parts of the hide. After that, three groups of four adjacent hide samples (10 cm × 10 cm) were cut from the back of the

treated hide. Brown lightproof plastic bottles were used as reaction vessels. Hide samples were put in the bottles, and the solutions of 50% of the hide sample weights were added respectively, containing FITC-labeled proteases with the same protein content of around 0.15 mg/mL. Then each mixture was adjusted to a certain pH value as required with sodium carbonate or formic acid solution. The bottles were put in a running drum for imitating the leather processing at the initial 25°C. Approximately 1 cm × 1 cm hide pieces from each hide sample were cut at intervals of 5 min, 1.0 h, 2.0 h, 3.0 h, 4.0 h, and 5.0 h, and immediately sampled and cut horizontally and longitudinally into sections of 20 μm with a freezing microtome (CM1950, Leica, Germany).

2.4 Confocal laser scanning microscopy analysis

The fluorescence of FITC was excited with an argon laser at a wavelength of 488 nm, and the fluorescence generated from FITC was colored green. According to the mice skin, where excitation maxima ranged from 295 to 360 nm[44], the mentioned excitation wavelength may be far from the wavelengths that could excite the auto-fluorescence originating from endogenous fluorophores found in the bovine hide, such as collagen, elastin, and aromatic amino acids. To investigate the protease permeation behaviors, including routes, directions, and depths of FITC-labeled proteases through the hide, the distribution of fluorescence on the hide longitudinal section surface was visualized using images in the *xy* plane. And the fluorescence distribution of the hide cross section was scanned from the hair follicle bottom to various depths through the *z-stack* plane. The confocal images were recorded and processed by the software on the confocal laser scanning microscope (Stellaris, Leica, American).

2.5 Quantitative analysis of permeation process and dehairing experiment

Sampling for quantitative analyses of the protease permeation processes from the hair side was carried out, simultaneously with the enzymatic dehairing experiments. The dehairing experiments also used the fleshed wet-salted bovine hide pretreated in the Permeation experiments section, and three groups of four adjacent hides (40 cm × 20 cm) were taken along the back line of the bovine hide. To each drum, 50% of water and a certain amount of unlabeled protease were added (based on the hide weight), and the added enzyme amount was calculated as the 100 U/mL of collagenolytic activity concentration of dehairing bath (based on the collagenolytic activity of P-U-B at pH 8.5, P-LKT-N at pH 7.5, and P-SG-B at pH 9.5, as well as 30 °C, respectively). Three proteases conducted the hair removal processes at the pH values consistent with their permeation experiments

with FITC-labeled proteases at the initial 25°C, and during each processing, the sampling intervals were the same as mentioned above. It should be noted that the animal hide is not uniform, and the structure of each hide layer is quite different. Thereafter, cross sections of sampled hides were immediately cut in increased depths from the hide surface to the hair follicle bottom, and every 400 μm was considered as a hide layer with permeated proteases.

The quantitative analysis results of permeation processes of unlabeled proteases were expressed as the protease amounts in the hide layers and hair as the time passed by for each dehairing pH condition, and the protease amounts in the hide layers and hair were calculated as the caseinolytic activity concentration per unit hide/hair weight. The caseinolytic activity concentrations of hide sections and hair samples at increasing times were determined, and the determinations were carried out according to the Proteolytic activity assay section with some modifications. Especially, the 1 mL of enzyme solution was replaced with 100 mg of hide sections and hair samples immersed in 1 mL of Britton-Robinson buffer at the corresponding pH (pH 8.5 for P-U-N, pH 7.5 for P-LKT-N, and pH 9.5 for P-SG-B), and the reaction time extended to 2 h at 30 °C. Unless otherwise indicated, a minimum of three replicate determinations were conducted in all experiments involving protease activity assay, and the results were expressed as the average ± standard deviation of replicate determinations. To determine the difference between groups, One-way ANOVA was performed with OriginPro 9.1 (Microcal, America), and the Tukey test was used to determine the significant differences between the means of the parameters. When $p < 0.05$, the difference is significant, when $p < 0.001$, the difference is extremely significant.

As soon as the hide pieces had been treated for 5 h, they were removed from the dehairing floats and their dehairing efficacy was visually evaluated by measuring the dehaired hide area. As well, the pelts were sequentially treated according to the conventional processes, and a stereoscopic microscope (TIPSCOPE, China) was used to observe the grain state of the finished crust leather.

3 Results and discussion

3.1 Purification and stability of FITC-labeled proteases

Three typical proteases with good dehairing ability, different molecular weights, and pI values were selected to be fluorescently labeled for permeation experiments, including two alkaline proteases, P-U-B and P-SG-B, and one neutral protease, P-LKN-N. The prepared fluorescently labeled protease solutions were likely to contain unbound fluorescein monomers and fluorescently labeled small-molecule non-enzyme proteins, which could enter

into the hide quickly, and interfere with observing the permeation of actual protease molecules into the hide, thus drawing incorrect conclusions. Crude FITC-labeled protease solutions were dialyzed to remove impurities, and the TLC was used to investigate the purification effect of dialysis. As shown in Fig. 2a, FITC monomers and labeled small-molecule non-enzyme proteins have significant migration, and the labeled target enzyme proteins with large molecule weights stay at the origin. The dialysis operation removes most of the small molecular impurities, and only target labeled proteases remain, hence, the interference from other substances can be eliminated in the following assessment of protease permeation behaviors.

To assess the stability of FITC-labeled proteases under enzymatic unhairing conditions, the dialyzed FITC-labeled protease solutions were incubated for 5 h at 30 °C and varying pH, and then spread out by TLC. As shown in Fig. 2b, all labeled proteases after dialysis stay at the origin, indicating that FITC monomer stably binds with protease molecules under the conditions of enzymatic unhairing.

3.2 UV-Vis and fluorescence spectroscopy characterizations of FITC-labeled proteases

The UV-Vis spectra were determined to confirm the formation of fluorescently labeled protease. Figure 3a is the plots of UV-Vis absorption spectra of the three FITC-labeled proteases in the wavelength range from 200 to 800 nm. It shows that all labeled proteases have similar absorption peaks. The characteristic absorption peak of FITC is known to locate at 490 nm, nevertheless, that of the FITC-labeled protease migrates to 494 nm, illustrating that FITC is well combined with the protease, which is consistent with the results reported in the literature[45].

The confocal observation is supposed to perform in a suitable fluorescence intensity and emission wavelength range. It is necessary to study the influence of pH on the fluorescence intensity and emission wavelength range of fluorescently labeled protease, thus suitable conditions are selected for confocal observation. Furthermore, the fluorescein contents of fluorescently labeled proteases need to be determined in the condition with a strong fluorescence intensity. Figure 3b shows the fluorescence intensity changes of FITC-labeled proteases with different pH values. The fluorescence is excited at 495 nm and its emission is collected between 505 and 600 nm. At different pH values, the fluorescence intensities of the FITC-labeled proteases vary considerably, but the peak location remains the same at 520 nm. Hence, the wavelength range of 505–555 nm is selected for the following confocal observation according to the confocal protocol and fluorescence intensity results to obtain strong fluorescence signals. Due to the highest fluorescence intensities of FITC-labeled proteases appearing at pH 9.5, thus, it should be better to determine the fluorescein content of FITC-labeled protease at this pH value.

3.3 Impact of fluorescent labeling on protease properties

The binding degree of fluorescein to protein is an important aspect to evaluate the fluorescent labeling result of protease, and the fluorescent labeling will cause some degree of change in enzyme characteristics. Generally, the higher the fluorescein binding degree to protein, the more protein properties change. Excessive fluorescently labeling may have a significant impact on the activity and solubility and even the molecule size and pI value of labeled protease molecule, making the labeled protease behave differently compared to the original protease in terms of permeation in the hide; while the fluorescence signal

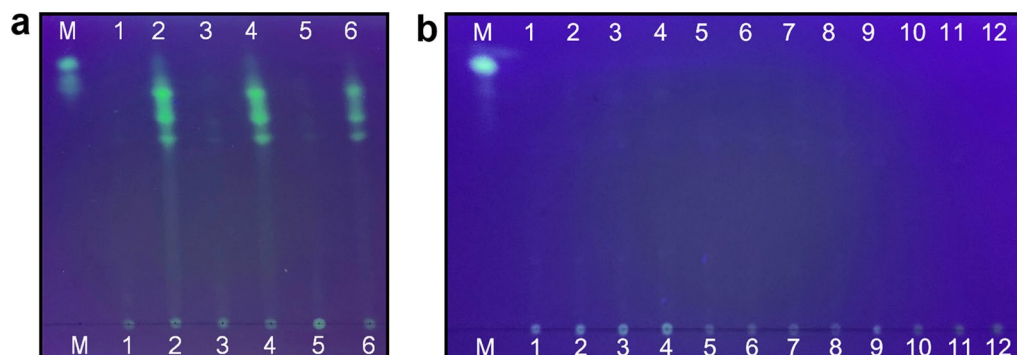


Fig. 2 Thin layer chromatography analysis results of FITC-labeled proteases. **a** Comparison between FITC-labeled proteases with and without dialysis: M—FITC monomer; 1/ 2—dialyzed/ undialyzed FITC-P-U-B; 3/ 4—dialyzed/ undialyzed FITC-P-LKT-N; 5/ 6—dialyzed/ undialyzed FITC-P-SG-B. **b** TLC diagram of FITC-labeled proteases incubated at different pH values and 30 °C for 5 h: M—FITC monomer; 1–4—FITC-P-U-B incubated at pH 7.5, 8.5, 9.5, and 10.5, respectively; 5–8/ 9–12—FITC-P-LKT-N/ FITC-P-SG-B incubated at pH 6.5, 7.5, 8.5, and 9.5, respectively

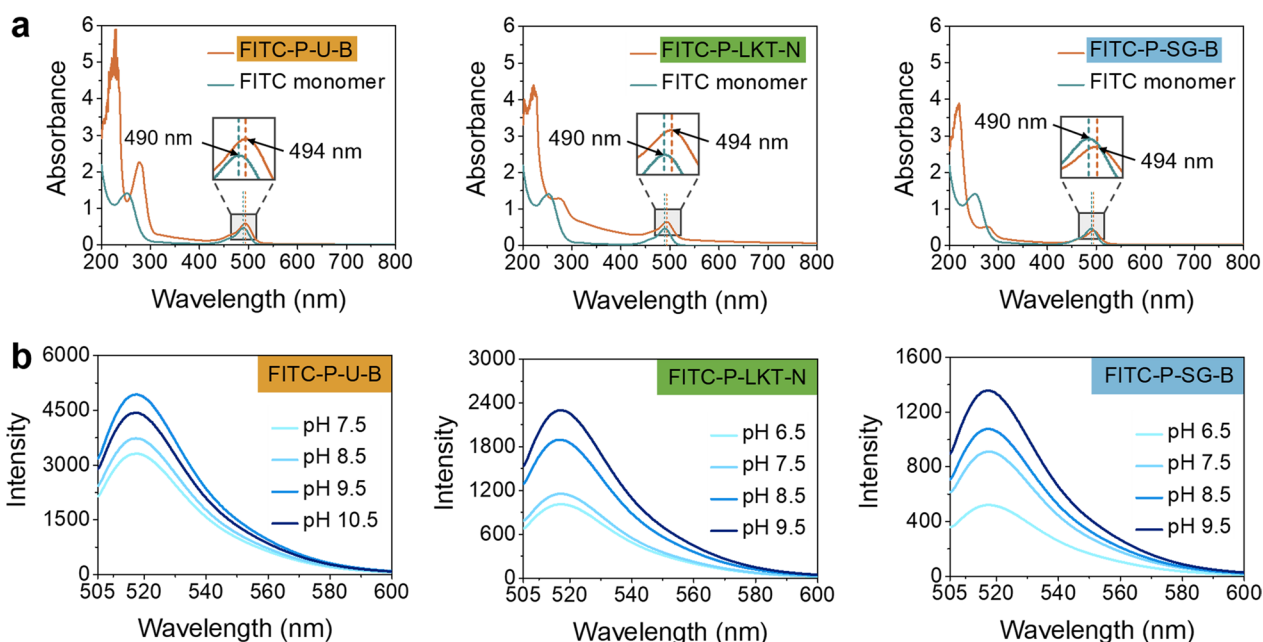


Fig. 3 Spectroscopy characterizations of FITC-labeled proteases. **a** UV-Vis spectra of FITC-labeled proteases. **b** Fluorescence spectra of FITC-labeled proteases at varying pH values

will be too weak to be detected if the binding degree of fluorescein to protein is too low. As the substitute for the original protease, the fluorescently labeled protease with an appropriate fluorescein binding degree to protein is crucial for investigating the permeation behaviors of protease. The labeled protease needs to be detectable by fluorescence signal, and the change in protease molecular characteristics should be as little as possible.

The permeation pre-experiments of proteases bound with different amounts of fluorescein showed that when the fluorescein binding degrees of FITC-P-U-B, FITC-P-LKT-N, and FITC-P-SG-B reached 0.018, 0.023, and 0.023, corresponding grams of fluorescein per gram of fluorescently labeled protein, respectively, the fluorescence signals of labeled proteases were obviously detected in the hide, and when the binding degree value was lower than these values, the fluorescence signal was not obvious. Therefore, 0.018, 0.023, and 0.023 were selected as the fluorescein binding degrees to protein to prepare the three fluorescently labeled proteases. Based on the above results, the impacts of fluorescent labeling on the protease characteristics, such as molecular weight, isoelectric point, and proteolytic activity, were further investigated under the appropriate binding degrees of fluorescein to protein.

3.3.1 Molecular weights and isoelectric points of FITC-labeled proteases

Fluorescent labeling may affect the molecular weight and isoelectric point of protease, which will also influence protease permeation behaviors in the hide. The electrophoresis analysis results show that the bands of the three FITC-labeled proteases on SDS-PAGE and IEF-PAGE almost have no change compared with their corresponding unlabeled proteases (Fig. 4a, and 4b). The FITC-P-U-B and FITC-P-SG-B, as well as their unlabeled proteases, appear as a single band of 25 kDa on SDS-PAGE; FITC-P-LKT-N and P-LKT-N exhibit several same bands on the gel, and the molecular weights of the two main protein components are 39 and 27 kDa, respectively (Fig. 4a). In the IEF-PAGE analysis, FITC-P-U-B, FITC-P-LKT-N, and FITC-P-SG-B, along with their unlabeled proteases, present a single band at 9.3, 8.4, and 7.0, respectively (Fig. 4b). It can be concluded that the purities of P-U-B and P-SG-B are high, and so are their FITC-labeled proteases. Nevertheless, there are several bands of P-LKT-N and its FITC-labeled protease on the SDS-PAGE gel but a single band on their IEF-PAGE gel. Therefore, the fluorescent labeling with the above selected binding degrees of fluorescein to protein does not exert a significant influence on the molecular weight and pI value of protease, indicating that the fluorescent labeling in this study will not

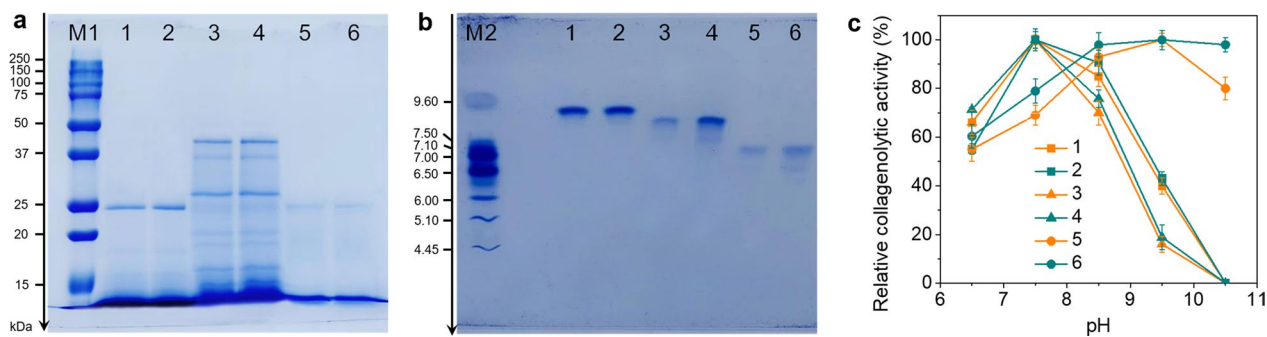


Fig. 4 Effect of fluorescent labeling on protease properties. **a** Molecular weights of FITC-labeled and unlabeled proteases by SDS-PAGE: M1—Molecular weight standard; 1/ 2—P-U-B/ FITC-P-U-B; 3/ 4—P-LKT-N/ FITC-P-LKT-N; 5/ 6—P-SG-B/ FITC-P-SG-B. **b** Isoelectric points of FITC-labeled and unlabeled proteases by IEF-PAGE: M2—Isoelectric point standard; the labels of 1–6 are the same as **a**. **c** Effect of pH on relative collagenolytic activities of proteases after fluorescent labeling (30°C): the labels of 1–6 are the same as **a**

Table 1 Proteolytic activities of FITC-labeled and unlabeled proteases (pH 8.0, 30°C)

Protease	Ca ¹ (U/mg)	Co ² (U/mg)	Co/Ca ³
P-U-B	772 ± 31	1750 ± 81	2.27 ± 0.12
FITC-P-U-B	818 ± 41	2360 ± 126	2.89 ± 0.15
P-LKT-N	1348 ± 87	2926 ± 198	2.17 ± 0.096
FITC-P-LKT-N	1111 ± 73	3039 ± 207	2.74 ± 0.13
P-SG-B	1246 ± 72	3071 ± 232	2.46 ± 0.30
FITC-P-SG-B	909 ± 62	3227 ± 222	3.55 ± 0.14

¹ Ca: Caseinolytic activity per unit mass protein

² Co: Collagenolytic activity per unit mass protein

³ Co/Ca: Collagenolytic activity per unit caseinolytic activity

interfere with the protease permeation behaviors in the hide in terms of size exclusion and charge properties.

3.3.2 Proteolytic activities of FITC-labeled proteases

Based on the selected fluorescein binding degree to protein mentioned above, the change in protease activity after being labeled, as well as the corresponding unlabeled proteases, were measured. As shown in Table 1, the collagenolytic activity per unit mass protein (Co) of the three labeled proteases only has a little bit of increment compared with the corresponding original proteases, as well as the caseinolytic activity per unit mass protein (Ca) of the labeled P-U-B after fluorescent labeling, but the Ca values of FITC-P-LKT-N and FITC-P-SG-B decrease somewhat. The values of collagenolytic activity per unit caseinolytic activity (Co/Ca) of these proteases increase after fluorescent labeling. The above results indicate that fluorescent labeling at the selected fluorescein binding degrees changes slightly the activities and specificities of the proteases and enhances their collagenolytic activities to a less extent. The reason may be that the isothiocyanate group in the FITC molecule

reacts with the amino group of the enzyme protein molecule, mainly the ϵ -amino group of lysine[45], and the slight alteration to the enzyme molecular structure leads to the changes in protease activity and specificity. Furthermore, the changes in the optimum pHs of the labeled proteases were also investigated. As shown in Fig. 4c, P-U-B, P-LKT-N, and P-SG-B exhibit maximum collagenolytic activity at pH 7.5, 7.5, and 9.5, respectively, and the optimum pHs of the labeled proteases almost have no change. Therefore, fluorescently labeled proteases can be used as substitutes for original proteases in permeation experiments.

3.4 Permeation behaviors of FITC-labeled proteases in the hide

Confocal laser scanning microscopy (CLSM) was used to investigate the permeation behaviors of FITC-labeled proteases in the hide. Confocal images of the three FITC-labeled proteases applied to the dehairing process of bovine hide at varying pH values are presented in Figs. 5, 6. As observed from the longitudinal sections of the hide in Fig. 5, the fluorescently labeled proteases gradually migrate into the hide as the increase of reaction time; the relative fluorescently labeled protease contents observed by relative fluorescence intensity are averagely higher near the hair side than the flesh layer, indicating that proteases penetrate through the hair side more easily. However, the permeation speed, depth, and distribution of the labeled proteases in different layers (represented by relative fluorescence intensity) are different with the change in pH value. As shown in Fig. 5a, FITC-P-U-B (pI 9.3) permeates into the hide faster and more deeply at pH 9.5 and 10.5 compared to that at pH 7.5 and 8.5; the labeled protease penetrates into the hide for around 1.25 mm from the hair side and reaches the position near the bottom of the hair follicle after 5 h at

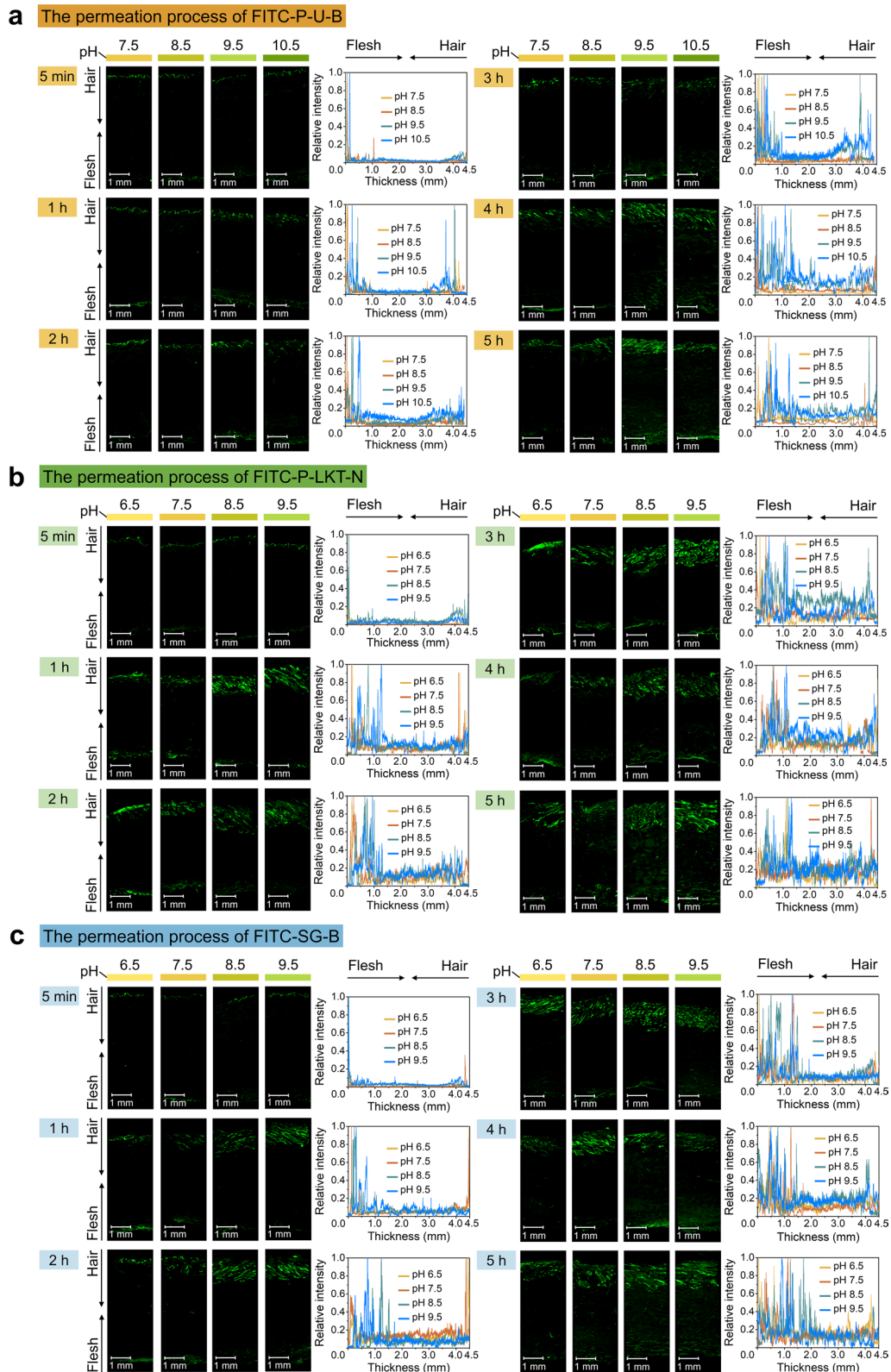


Fig. 5 Confocal xy images and corresponding relative fluorescence intensity analyses of longitudinal sections obtained from the application of FITC-P-U-B (a), FITC-P-LKT-N (b), and FITC-SG-B (c) at different pH values and timings (5 min, 1 h, 2 h, 3 h, 4 h, and 5 h)

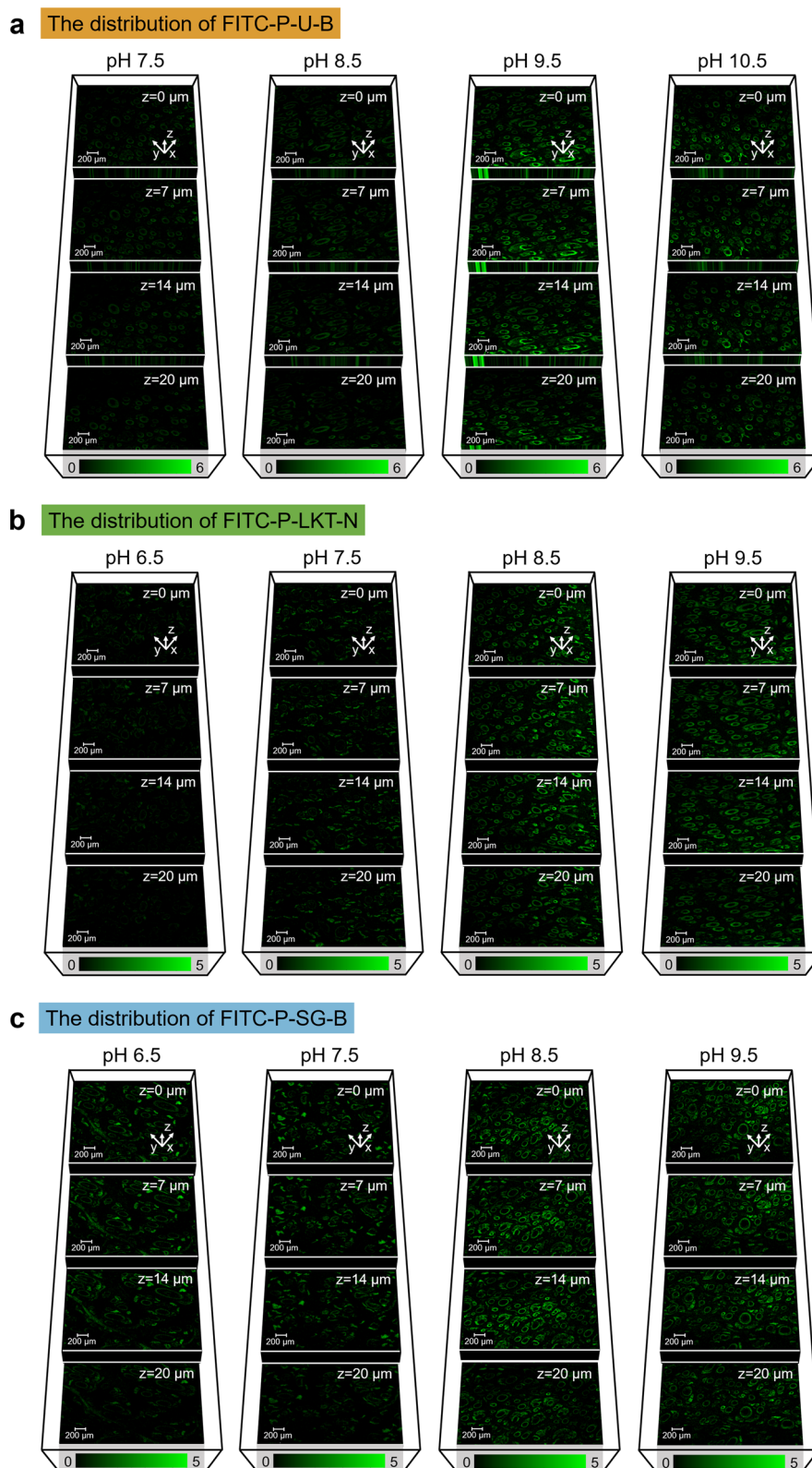


Fig. 6 Confocal z-stack images of cross sections near the hair follicle bottom obtained from the application of FITC-P-U-B (a), FITC-P-LKT-N (b), and FITC-P-SG-B (c) at different pH values and 5 h with 0 μm , 7 μm , 14 μm , and 20 μm depths from the surface of hide cross section, respectively

higher pH values (pH 9.5 and 10.5), while the protease is detected in the area less than 0.5 mm from the superficial layer at lower pH values (pH 7.5 and 8.5), suggesting that the labeled protease is more permeable in the hide when applied at higher pH values. Analogously, the permeation behaviors of FITC-P-LKT-N (pI 8.4) at varying pH values are more similar to that of FITC-P-U-B compared with FITC-P-SG-B as shown in Fig. 5b and 5c, but its permeation depth is deeper than that of FITC-P-U-B; the permeation speed of FITC-P-LKT-N is faster and the fluorescence intensity near the hair follicle bottom is stronger at higher pHs (8.5 and 9.5) than low pHs (6.5 and 7.5). As far as FITC-P-SG-B (pI 7.0), it is more easily to penetrate into the hide for around 1.5 mm from the hair side, and the penetrating depth and speed do not exhibit significant difference at pH values of more than 7.5, as shown in Fig. 5c; while the labeled protease gets lodged into the upper layer with the depth of around 1.0 mm at pH 6.5, deeper than that of FITC-P-U-B. The

reasons for the change in protease permeation behaviors with varying pHs will be explained later.

A typical permeation process of fluorescently labeled protease is exhibited in Fig. 7a, and the images are from the superimposition of fluorescence and optical microscopy photos, mainly showing histological sections of hair follicles and their surrounding areas. It can be seen that at the beginning of protease permeation (5 min), the hair follicular infundibulum, the upper part of the hide and hair follicle, shows a rather strong fluorescence intensity, indicating that the labeled protease is absorbed by the hide surface. As time goes on, the labeled protease mainly migrates along the hair follicle to the deeper layer. The superimposed image of 2 h of protease permeation does not reveal the intact hair follicle structure due to the direction of hair growth, no fluorescence signal is detected in some hair root sheaths located in the deeper layer, and the fluorescence intensity decreases along the hair follicle

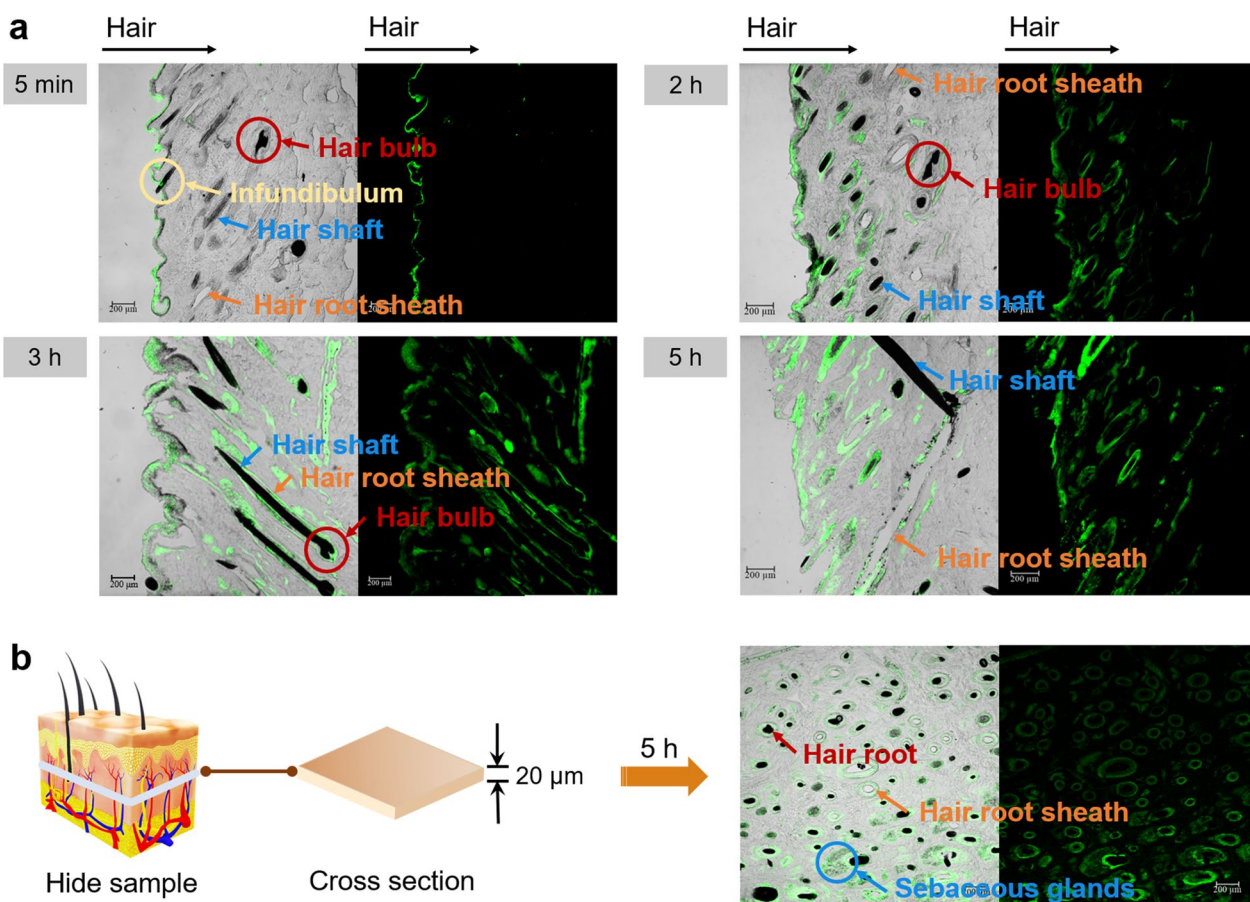


Fig. 7 Superimposition of fluorescence and optical microscopy images of longitudinal and cross sections. **a** A typical permeation process of the FITC-labeled protease exhibited by the superimposition of fluorescence and optical microscopy photos (red arrows refer to the hair bulb, blue arrows refer to the hair shaft, orange arrows refer to the hair root sheath, and yellow arrows refer to the hair infundibulum). **b** A cross section with the permeated FITC-labeled protease exhibited by the superimposition of fluorescence and optical microscopy photos (red arrows refer to the hair root, blue arrows refer to the sebaceous gland, and orange arrows refer to the hair root sheath)

direction, indicating that only a small amount of labeled protease reaches the follicle bottom. It needs about 3 h for the FITC-labeled protease to penetrate a depth of the total hair follicle length and reach the bottom of the hair bulb. The permeation depth and relative fluorescence intensity around the hair follicle have not seemed to change much as time further passes. It is worth noting that the fluorescence image of the upper hide layer is still not intact and continuous, and the fluorescence signal is mainly around hair follicles with a little diffusion as the further extension of permeation time to 5 h. Hence, it can be inferred that the main route of protease permeating into the hide is the transfollicular way. Due to the special structure of the hair infundibulum, both a reservoir structure and an interrupted barrier, it is more permeable than the interfollicular epidermis and the superficial part of the infundibulum, and the hair infundibular corneocytes are smaller and crumblier than the horny layer of the interfollicular epidermis and the superficial part of the infundibulum whose cells are intact and relatively impermeable[35]. Therefore, it is reasonable to conclude that due to the proteolytic action of protease on hair infundibular corneocytes, the protease begins to spread to deeper hide layers through hair follicles, and this may be the reason why the fluorescence signal is mainly around hair follicles with a little diffusion at 5 h of protease permeation. As mentioned above, FITC signals also could be detected on the flesh layer of hide with relatively lower fluorescence intensity distribution, though the flesh side does not possess hair follicles or other skin appendages. These results suggest that the transfollicular pathway is the main protease permeation; although the interfibrillar pathway also exists, it does not play an important role.

Figure 6 shows the z-stack confocal images obtained from cross sections with a thickness of 20 μm at the hair follicle bottom, and these cross sections are investigated to further confirm the permeation depths and routes of FITC-labeled proteases at different pH values from other perspectives. Fluorescence signals can be detected around the hair, as well as the hair root sheath and sebaceous gland, exhibiting different circles (Fig. 7b), which confirms that fluorescently labeled proteases mainly migrate along the hair follicle to the deep layer as observed in longitudinal sections. As is apparent from the results in Fig. 6a, 6b, and 6c, fluorescence intensities are much stronger in the deeper layers of the hide treated with FITC-labeled proteases at a high pH than low pH, especially when the pH is higher than the pI value of FITC-labeled protease, suggesting they can more easily permeate through deeper hide layers instead of accumulated in the superficial areas of hide at high pH values.

3.5 Quantitative analyses of protease permeation processes and enzymatic dehairing effectiveness

Permeation experiments of fluorescently labeled proteases visually exhibited the permeation routes and directions of proteases, and the differences in the permeation rates and depths of proteases at varying pH values. Quantitative analyses of protease permeation behaviors in the hide were further conducted, and the relations between the permeation behaviors and dehairing effects of proteases were also investigated.

The permeation experiments of labeled and unlabeled proteases are conducted at the dosages of the same enzyme protein amount, and the fluorescently labeled and the corresponding unlabeled protease have similar molecular weight and pI according to the previous characterization determination results, therefore, they should have the similar permeation behaviors in the hide.

Hide pieces were dehaired with P-U-B, P-LKT-N, and P-SG-B, respectively, and the sampling intervals were the same as mentioned above. Cross sections of sampled hides were immediately split in increased depths from the upper hide surface to the hair follicle bottom, and every layer with 400 μm thickness (20 slices) was considered as one hide layer containing permeated proteases. The hide from the surface of the epidermis to the bottom of the hair follicle was divided into two layers. The upper hide layer with 400 μm thickness consisted of the epidermis layer and upper grain layer, while the deeper hide layer with 400 μm thickness was the deeper grain layer containing hair follicles, which ended at the bottoms of hair follicles. The amount of the protease permeating in different hide layers was expressed in the caseinolytic activity of protease per mg of the hide (U/mg), which represented the relatively average amount of the protease arriving at the hide layer. The results of the protease permeating in different hide layers at varying pH values as time increases and the change trends are given in Fig. 8.

As shown in Fig. 8a, 8b, and 8c, the amount of protease absorbed by the hair and permeating into different hide layers increases with the extension of time in the first 120 min, then increases slowly and tends to be stable. In the process of enzyme treatment, the protease content in the hair and upper grain layer, especially in the upper grain layer, is generally higher than that in the deeper grain layer, which is consistent with the permeation behaviors of FITC-labeled proteases in the hide, indicating that the protease concentration decreases along the direction of the hair follicle. The adsorption of protease by the hair and collagen in the grain layer is greatly influenced by the pH values, as well as the permeation of protease in the hide. When the enzyme concentration in the upper grain layer is high, the enzyme concentration in the deeper layer is low, namely, the strong affinity between

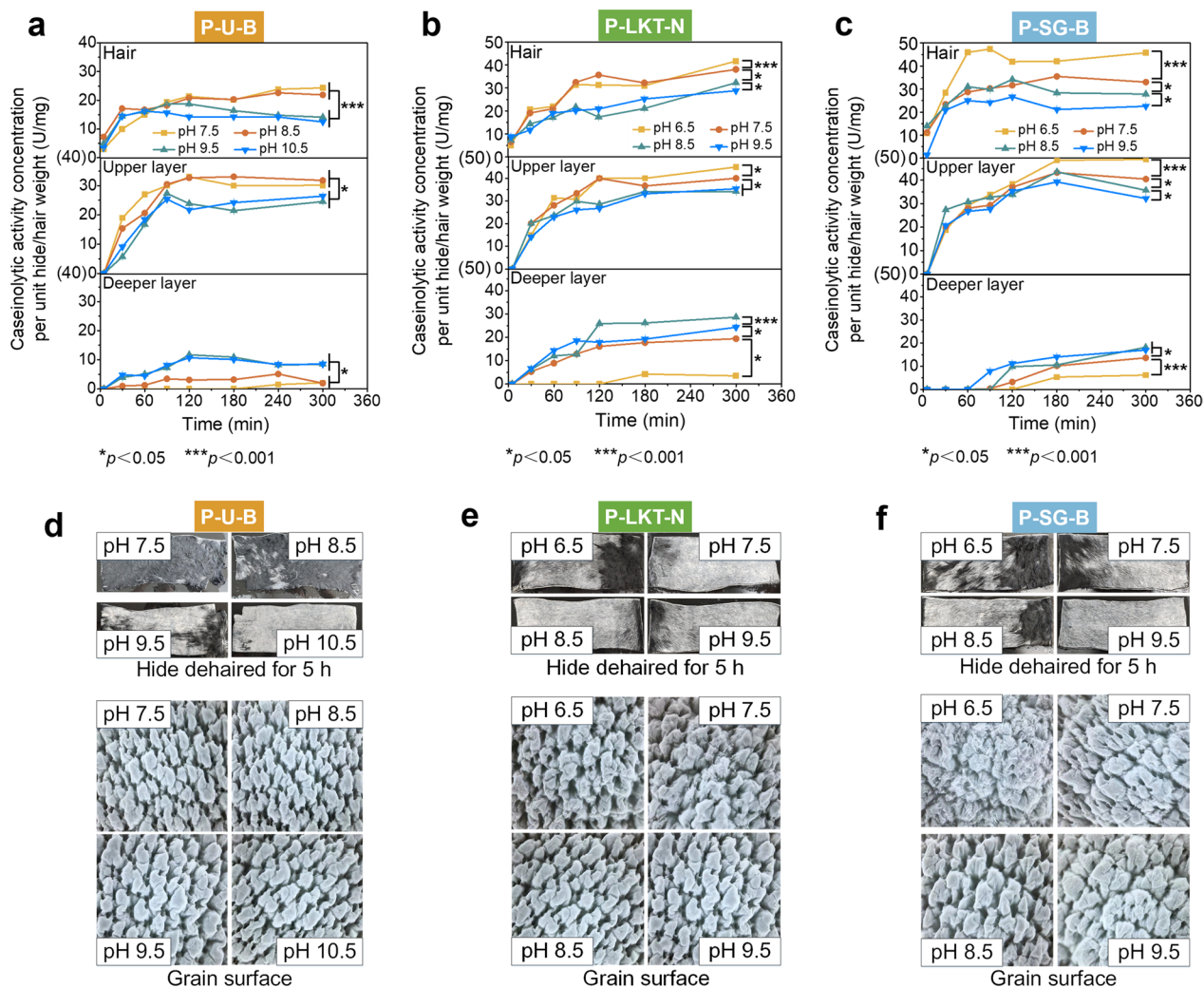


Fig. 8 Quantitative analyses of protease permeation processes and corresponding enzymatic dehairing results. The amount of P-U-B (a), P-LKT-N (b), and P-SG-B (c) absorbed by the hair and permeating into different hide layers at varying pH values. Images of bovine hides dehairing by P-U-B (d), P-LKT-N (e), and P-SG-B (f) obtained from 5 h and the corresponding crust leather grain surface

the protease and hide surface makes the permeability of protease in the hide poor, and results in the decrease of enzyme concentration in the deeper hide layer. The absorbing property of enzyme by the collagen and keratin is obviously affected by the pH value. In Fig. 8a, the protease concentration of P-U-B is much higher in the deeper grain layer with a significant difference ($p < 0.05$) at pH 9.5 and 10.5 than at pH 7.5 and 8.5. Since this layer is close to the bottom of the hair follicle, the more protease permeated permeating here is conducive to the hydrolysis of junction proteins between the hair bulb and hair papilla, consequently achieving hair removal. The protease concentration of P-U-B in the deeper layer is significantly higher at pH 7.5 and 8.5 than at pH 9.5 and 10.5 ($p < 0.05$); the adsorption ability of P-U-B by the hair

is also higher at lower pH values than that at higher pH values (pH 9.5 and 10.5), and the difference is very significant ($p < 0.001$). Similarly, the effect of pH on the adsorption ability by the hair/hide surface and the permeation behaviors in the hide of P-LKT-N (Fig. 8b) and P-SG-B (Fig. 8c) is similar to that of P-U-B, which is consistent with the permeation behaviors of FITC-labeled proteases in the hide. Namely, the protease concentration in the deeper hide is significantly higher at high pH than that at low pH, especially when the pH is higher than the pI of protease.

The dehairing states of bovine hides at 5 h and the corresponding grain morphology of crust leather pieces are shown in Fig. 8d, 8e, and 8f. In Fig. 8d, under the same protease dosage, P-U-B dehairsts faster and more easily at

pH 9.5 and 10.5 than that at pH 7.5 and 8.5, especially at pH 10.5, while the protease hardly dehairst at pH 7.5 and 8.5, though the proteolytic activity is quite low at pH 10.5 (seen in Fig. 4c), which is consistent with the permeability of enzyme, i.e. when the protease easily reaches the bottom of the hair follicle, and more enzymes accumulate at the area (seen in Fig. 5a), the hair removal becomes easy. Moreover, the grain surface treated by P-U-B at pH 9.5 and 10.5 is better than that at pH 7.5 and 8.5, indicating the protease accumulates little on the grain surface at high pH values. As for P-LKT-N, it is the same case. It can be seen in Fig. 8e that the dehairing effectiveness of P-LKT-N is the best at the low pH of 8.5, even though the proteolytic activity of the protease at pH 8.5 is lower than that at pH 6.5 and 7.5 (seen in Fig. 4c), but there is more enzyme accumulating in the deeper layer at pH 8.5. In addition, the surface of the grain layer treated by P-LKT-N at pH 6.5 and 7.5 is damaged to some extent, and it is intact at pH 8.5 and 9.5. It can be attributed that the protease cannot easily penetrate the hide at a low pH, and a long-time accumulation on the grain results in the excessive proteolysis of the grain layer. Figure 8f shows that the best hair removal effectiveness of P-SG-B also happens at the high pH of 9.5, and the unhairing effectiveness improves with the increase of proteolytic activity resulting from the rise of pH. It can also be seen that the grain surfaces of hides are also damaged by the protease at lower pH values, especially at pH 6.5, which also indicates that the protease is not easy to penetrate the hide at a low pH resulting in excessive hydrolysis of the grain protein on the surface because of the long duration. Based on the above results, it can be concluded that the dehairing effects and grain damages of proteases are not fully consistent with their corresponding proteolytic activities, but more consistent with the permeation behaviors of proteases in the hide, and the permeation behaviors of proteases are significantly influenced by the charge properties of hide collagen and enzyme molecules depending on pI values of the two kinds of proteins and the applying pH values, which will be illustrated later.

3.6 Mechanism of charge regulation of protease permeation behaviors into the hide

According to the permeation experiment results of fluorescently labeled and unlabeled proteases, it is found that the permeation behaviors of proteases into the hide are greatly impacted by the charge states of hide protein and protease molecules, which depends on the pI of proteins and the pH of the solution. At high pH values, especially when the pH value is higher than the pI value of protease, the protease can easily penetrate into the hide, achieving a faster permeation rate and deeper permeation depth. Since the main components of proteases and

hair/hide layers are proteins, which are amphoteric compounds, the surface charges of proteases and hair/hide layers are determined by the pI values of proteins and the pH value of the solution under certain environmental conditions (such as ionic strength and temperature). The electrostatic interaction between the surface charges of enzyme molecules and hide layers has an important effect on protease permeation behaviors in the hide. It is known that the hair follicle is a depression formed by the epidermis into the dermis, and the main component of hair and epidermis is keratin, while the main component of the grain layer beneath the epidermis is collagen. The pI of hair keratin is 4.3–5.9[46], that of epidermis keratin is 5.05[47], and that of hide collagen is 7.0–8.0[48]. The enzymatic dehairing pH range of 6.5–10.5 is higher than the pI value of keratin in the hair, epidermis, and hair follicle, so they are all negatively charged, whereas P-U-B (pI 9.3), P-LKT-N (pI 8.4), and P-SG-B (pI 7.0) can be positively charged ($\text{pH} < \text{pI}$), close to uncharged ($\text{pH} \approx \text{pI}$), and negatively charged ($\text{pH} > \text{pI}$). The mechanism of charge regulation of protease permeation behaviors into the animal hide is as follows (Fig. 9). When the pH of the solution is lower than the pI of the protease, the positively charged protease rapidly binds to the negatively charged hair and epidermis due to the electrostatic attraction, and accumulates a large amount on the epidermis and grain surface, making it difficult to penetrate further into the deeper hide. As time goes on, only a small number of proteases can reach the hair follicle bottom along the hair follicle. Therefore, the protease has a weak hydrolysis effect on the junction protein between the hair bulb and hair papilla, resulting in slow hair removal speed, poor effect, and damaged grain. When the pH of the solution is near or higher than the pI of the protease, keratin, and collagen, only a small amount of negatively charged or barely charged proteases stays in the epidermis layer and grain surface due to the electrostatic repulsion or weak electrostatic interaction. Driven by mechanical forces, the protease can easily permeate through the negatively charged epidermis and upper grain layer along the hair follicle and arrive at the bottom of the hair bulb, thus the efficient and rapid hair removal and weakened proteolysis of grain surface can be achieved.

4 Conclusion

To sum up, in the design of traditional enzymatic dehairing in the leather process, the influence of dehairing pH on the enzyme activity usually gets more attention but its influence on the enzyme permeability in the hide is ignored. Therefore, the problem of slow hair removal speed and serious damage to the hide grain surface in the biological leather hair removal technology has not been solved. To solve

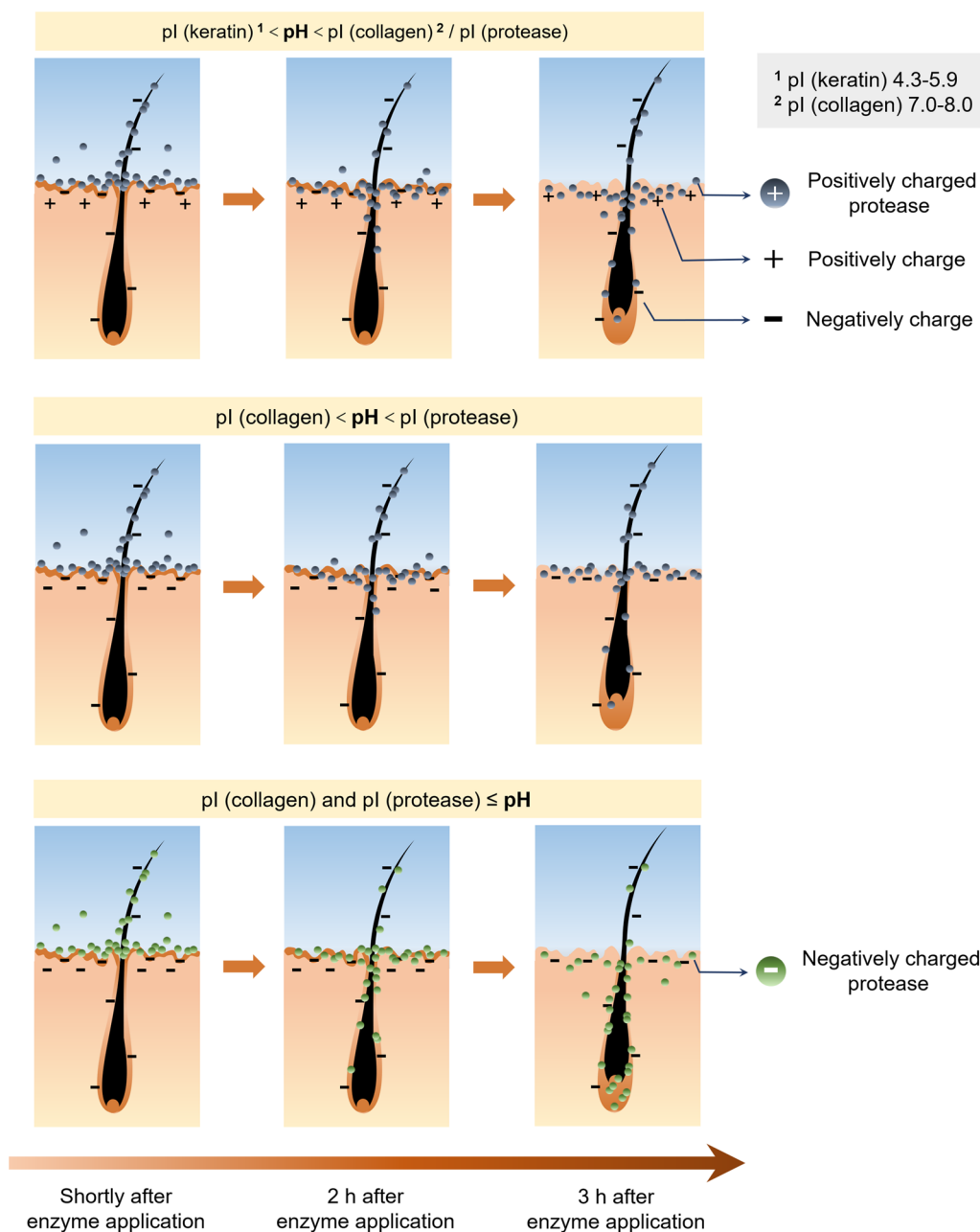


Fig. 9 Mechanism of charge regulation of protease permeation behaviors into the animal hide

this problem, the permeation behavior and influence mechanism of protease in the hide were studied. The results show that the protease is more likely to permeate into the hide through the hair side during the enzymatic dehairing process, and the main permeation route is the transfollicular way. The permeation behaviors of proteases largely depend on the effect of pH on the surface charges of proteases and hair/hide layers,

thus influencing the electrostatic interaction between them during the protease permeation into the hide. The mechanism of improving permeation processes of proteases into the animal hide based on the charge adjustment provides a theoretical basis for the design and development of efficient enzymatic dehairing technology, furthermore, this mechanism also can be used in other processes involving enzyme application in the leather industry.

Acknowledgements

We thank Qingshuang Song, Zhonghui Wang, and Jinwei Zhang for their technical help at Sichuan University.

Author contributions

MG conceived the idea, performed the experiments, analyzed the data, and drafted the manuscript. JS, XZ, and CZ analyzed and validated the data. BP conceived the idea, supervised the project, and revised the manuscript. SAC revised the manuscript. All authors read and approved the final manuscript.

Funding

This work was financially supported by National Key R&D Program of China (2017YFB0308402).

Availability of data and materials

The datasets used and/or analyzed during the current study are available from the corresponding author on reasonable request.

Declarations

Competing interests

The authors declare that they have no competing interests.

Author details

¹National Engineering Research Center of Clean Technology in Leather Industry, Sichuan University, Chengdu 610065, China. ²Present Address: Key Laboratory of Leather Chemistry and Engineering of Ministry of Education, Sichuan University, Chengdu 610065, China. ³Department of Leather and Fiber Technology, University of Veterinary and Animal Sciences, Lahore 54000, Pakistan.

Received: 2 December 2022 Revised: 21 February 2023 Accepted: 3 March 2023

Published online: 16 March 2023

References

- Hasan MJ, Haque P, Rahman MM. Protease enzyme based cleaner leather processing: A review. *J Clean Prod.* 2022;365:132826. <https://doi.org/10.1016/j.jclepro.2022.132826>.
- Su C, Gong J, Qin J, Li H, Li H, Xu Z, Shi J. The tale of a versatile enzyme: Molecular insights into keratinase for its industrial dissemination. *Biotechnol Adv.* 2020;45:107655. <https://doi.org/10.1016/j.biotechadv.2020.107655>.
- Qiu J, Wilkens C, Barrett K, Meyer AS. Microbial enzymes catalyzing keratin degradation: Classification, structure, function. *Biotechnol Adv.* 2020;44:107607. <https://doi.org/10.1016/j.biotechadv.2020.107607>.
- Hassan MA, Abol-Fotouh D, Omer AM, Tamer TM, Abbas E. Comprehensive insights into microbial keratinases and their implication in various biotechnological and industrial sectors: a review. *Int J Biol Macromol.* 2020;154:567–83. <https://doi.org/10.1016/j.ijbiomac.2020.03.116>.
- Sujitha P, Kavitha S, Shakilanishi S, Babu NKC, Shanthi C. Enzymatic dehairing: a comprehensive review on the mechanistic aspects with emphasis on enzyme specificity. *Int J of Biol Macromol.* 2018;118:168–79. <https://doi.org/10.1016/j.ijbiomac.2018.06.081>.
- Baba HAME, Covington AD, Davighi D. The effects of hair shaving on unhairing reactions—Part 2: a new mechanism of unhairing. *J Soc Leath Tech Ch.* 2000;84(1):48–53.
- Liya SM, Umesh M, Nag A, Chinnathambi A, Alharbi SA, Jhanani GK, Shanmugam S, Brindhadevi K. Optimized production of keratinolytic proteases from *Bacillus tropicus* LS27 and its application as a sustainable alternative for dehairing, destaining and metal recovery. *Environ Res.* 2023;221:115283. <https://doi.org/10.1016/j.envres.2023.115283>.
- Li X, Zhang S, Zhang Q, Gan L, Jiang G, Tian Y, Shi B. Characterization and application of a novel halotolerant protease with no collagenase activity for cleaner dehairing of goatskin. *Process Biochem.* 2022;113:203–15. <https://doi.org/10.1016/j.procbio.2022.01.006>.
- Sujitha P, Shanthi C. Insights into substrate specificity of proteases for screening efficient dehairing enzymes. *Int J Biol Macromol.* 2021;172:360–70. <https://doi.org/10.1016/j.ijbiomac.2021.01.065>.
- Tian J, Long X, Tian Y, Shi B. Eco-friendly enzymatic dehairing of goatskins utilizing a metalloprotease high-effectively expressed by *Bacillus subtilis* SCK6. *J Clean Prod.* 2019;212:647–54. <https://doi.org/10.1016/j.jclepro.2018.12.084>.
- Yates JR. Studies in depilation. Part X. The mechanism of the enzyme depilation process. *J Soc Leath Tech Ch.* 1972(56):158–75.
- Ma J, Hou X, Gao D, Zhang J. Diffusion and reaction behavior of proteases in cattle hide matrix via FITC labeled proteases. *J Am Leather Chem As.* 2014;109:138–43.
- Yang Q, Zeng Y, Zhang W, Liao X, Shi B. Investigation of mass transfer characteristics of protease in bating process using fluorescence tracing. *Chin Leather.* 2015;44:16–9.
- Luo F, Zhong X, Gao M, Peng B, Long Z. Progress and mechanism of breaking glycoconjugates by glycosidases in skin for promoting unhairing and fiber opening-up in leather manufacture. A review. *J Leather Sci Eng.* 2020;2(1):1–16. <https://doi.org/10.1186/s42825-020-00025-0>.
- Song Y, Wu S, Yang Q, Liu H, Zeng Y, Shi B. Factors affecting mass transfer of protease in pelt during enzymatic bating process. *J Leather Sci Eng.* 2019. <https://doi.org/10.1186/s42825-019-0007-7>.
- Zeng Y, Yang Q, Wang Y, Zhou J, Shi B. Neutral protease assisted low-sulfide hair-save unhairing based on pH-sensitivity of enzyme. *J Am Leather Chem Assoc.* 2016;111:345–53.
- Elmowafy M. Skin penetration/permeation success determinants of nanocarriers: Pursuit of a perfect formulation. *Colloids Surf B: Biointerfaces.* 2021;203:111748. <https://doi.org/10.1016/j.colsurfb.2021.111748>.
- Nava-Arzaluz MG, Piñón-Segundo E, Ganem-Rondero A. Chapter 11 - Lipid nanocarriers as skin drug delivery systems. *Nanoparticles in Pharmacotherapy.* Cambridge, American: Elsevier Inc.; 2019: 311–90. <https://doi.org/10.1016/C2017-0-04569-X>.
- Elmowafy M, Shalaby K, Ali HM, Alruwaili NK, Salama A, Ibrahim MF, Akl MA, Ahmed TA. Impact of nanostructured lipid carriers on dapsone delivery to the skin: in vitro and in vivo studies. *Int J Pharm.* 2019;572:118781. <https://doi.org/10.1016/j.ijpharm.2019.118781>.
- Wu X, Landfester K, Musyanovych A, Guy RH. Disposition of charged nanoparticles after their topical application to the skin. *Skin Pharmacol Physiol.* 2010;23:117–23. <https://doi.org/10.1159/000270381>.
- Rosado C, Silva C, Reis CP. Hydrocortisone-Loaded poly(ϵ -caprolactone) nanoparticles for atopic dermatitis treatment. *Pharm Dev Technol.* 2013;18:710–8. <https://doi.org/10.3109/10837450.2012.712537>.
- Siddique MI, Katas H, Amin MCIM, Ng S, Zulfakar MH, Jamil A. *In-vivo* dermal pharmacokinetics, efficacy, and safety of skin targeting nanoparticles for corticosteroid treatment of atopic dermatitis. *Int J Pharm.* 2016;507:72–82. <https://doi.org/10.1016/j.ijpharm.2016.05.005>.
- Ogiso T, Yamaguchi T, Iwaki M, Tanino T, Miyake Y. Effect of positively and negatively charged liposomes on skin permeation of drugs. *J Drug Target.* 2001;9:49–59. <https://doi.org/10.3109/10611860108995632>.
- Tupal A, Sabzichi M, Ramezani F, Kouhsoltani M, Hamishehkar H. Dermal delivery of doxorubicin-loaded solid lipid nanoparticles for the treatment of skin cancer. *J Microencapsul.* 2016;33:372–80. <https://doi.org/10.1080/02652048.2016.1200150>.
- Vedadghavami A, Zhang C, Bajpayee AG. Overcoming negatively charged tissue barriers: drug delivery using cationic peptides and proteins. *Nano Today.* 2020;34:100898. <https://doi.org/10.1016/j.nantod.2020.100898>.
- Divya G, Panonnummal R, Gupta S, Jayakumar R, Sabitha M. Acitretin and aloe-emodin loaded chitin nanogel for the treatment of psoriasis. *Eur J Pharm Biopharm.* 2016;107:97–109. <https://doi.org/10.1016/j.ejpb.2016.06.019>.
- Jung S, Otberg N, Thiede G, Richter H, Sterry W, Panzner S, Lademann J. Innovative liposomes as a transfollicular drug delivery system: penetration into porcine hair follicles. *J Invest Dermatol.* 2006;126:1728–32. <https://doi.org/10.1038/sj.jid.5700323>.
- Zhang Y, Jing Q, Hu H, He Z, Wu T, Guo T, Feng N. Sodium dodecyl sulfate improved stability and transdermal delivery of salidroside-encapsulated niosomes via effects on zeta potential. *Int J Pharm.* 2020;580:119183. <https://doi.org/10.1016/j.ijpharm.2020.119183>.
- Kohli AK, Alpar HO. Potential use of nanoparticles for transcutaneous vaccine delivery: effect of particle size and charge. *Int J Pharm.* 2004;275:13–7. <https://doi.org/10.1016/j.ijpharm.2003.10.038>.

30. Wang Y, Hu L. Essential role of isoelectric point of skin/leather in leather processing. *J Leather Sci Eng.* 2022;25(4):1–3. <https://doi.org/10.1186/s42825-022-00099-y>.
31. Alexander A, Dwivedi S, Ajazuddin, Giri TK, Saraf S, Saraf S, Tripathi DK. Approaches for breaking the barriers of drug permeation through transdermal drug delivery. *J Control Release.* 2012;164:26–40. <https://doi.org/10.1016/j.jconrel.2012.09.017>.
32. Krishnan V, Mitragotri S. Nanoparticles for topical drug delivery: potential for skin cancer treatment. *Adv Drug Deliver Rev.* 2020;153:87–108. <https://doi.org/10.1016/j.addr.2020.05.011>.
33. Cantera CS, Goya L, Garro ML, Babeito C, Galarza B. Hair saving unhairing process. Part 6 Stratum corneum as a diffusion barrier: Chemical-Mechanical injury of epidermis. *J Soc Leath Tech Ch.* 2004;88:121–30.
34. Abdel-Hafez SM, Hathout RM, Sammour OA. Tracking the transdermal penetration pathways of optimized curcumin-loaded chitosan nanoparticles via confocal laser scanning microscopy. *Int J Biol Macromol.* 2018;108:753–64. <https://doi.org/10.1016/j.ijbiomac.2017.10.170>.
35. Patzelt A, Knorr F, Blume-Peytavi U, Sterry W, Lademann J. Hair follicles, their disorders and their opportunities. *Drug Discov Today.* 2008;5(2):e173–81. <https://doi.org/10.1016/j.ddmec.2008.04.006>.
36. Lauer AC, Ramachandran C, Lieb LM, Niemiec S, Weiner ND. Targeted delivery to the pilosebaceous unit via liposomes. *Adv Drug Deliver Rev.* 1996;18(3):311–24. [https://doi.org/10.1016/0169-409X\(95\)00089-P](https://doi.org/10.1016/0169-409X(95)00089-P).
37. Meidan VM. Methods for quantifying intrafollicular drug delivery: a critical appraisal. *Expert Opin Drug Del.* 2010;7(9):1095–108. <https://doi.org/10.1517/17425247.2010.503954>.
38. Liu C, Chen X, Zeng Y, Shi B. Effect of the surface charge of the acid protease on leather bating performance. *Process Biochem.* 2022;121:330–8. <https://doi.org/10.1016/j.procbio.2022.07.023>.
39. Tian Q, Zhang C, Wang X, Wang W, Huang W, Cha R, Wang C, Yuan Z, Liu M, Wan H, et al. Glycyrhretinic acid-modified chitosan/poly(ethylene glycol) nanoparticles for liver-targeted delivery. *Biomaterials.* 2010;31:4748–56. <https://doi.org/10.1016/j.biomaterials.2010.02.042>.
40. Redmile-Gordon MA, Armenise E, White RP, Hirsch PR, Goulding KWT. A comparison of two colorimetric assays, based upon Lowry and Bradford techniques, to estimate total protein in soil extracts. *Soil Biol Biochem.* 2013;67:166–73. <https://doi.org/10.1016/j.soilbio.2013.08.017>.
41. Laemmli UK. Cleavage of structural proteins during the assembly of the head of *Bacteriophage T4*. *Nature.* 1970;227:680–5.
42. Errasti ME, Caffini NO, López LMI. Proteolytic extracts of three *Bromeliaceae* species as eco-compatible tools for leather industry. *Environ Sci Pollut R.* 2018;25:21459–66. <https://doi.org/10.1007/s11356-017-1096-6>.
43. Gao M, Zhang X, Tian Y, Zhang C, Peng B. Development and validation of a label-free method for measuring the collagen hydrolytic activity of protease. *Bioproc Biosyst Eng.* 2021;44(12):2525–39. <https://doi.org/10.1007/s00449-021-02624-5>.
44. Drakaki E, Borisova E, Makropoulou M, Avramov L, Serafetinides AA, Angelov I. Laser induced autofluorescence studies of animal skin used in modeling of human cutaneous tissue spectroscopic measurements. *Skin Res Technol.* 2007;13(4):350–9. <https://doi.org/10.1111/j.1600-0846.2007.00237.x>.
45. Liu AP. *Fluorescence principles and practice for cell biology*. 1st ed. Hefei, China: Press of University of Science and Technology of China; 2007.
46. Yan P, Xu J, Zhao Z, Guo C, He G. Isoelectric focusing analysis of human and animal hair keratins. *Chin J Forensic Med.* 1992;7(2):80–3.
47. Liu S, Tao J, Zhao G, Zhao X, Yang Y. Differential proteomic analysis of milk in the postpartum period of Holstein cows. *J Gansu Agric Univ.* 2016:7–13.
48. Yue X. *Processing of Animal Food*. Beijing, China: China Light Industry Press; 2014.

Publisher's Note

Springer Nature remains neutral with regard to jurisdictional claims in published maps and institutional affiliations.

Submit your manuscript to a SpringerOpen[®] journal and benefit from:

- Convenient online submission
- Rigorous peer review
- Open access: articles freely available online
- High visibility within the field
- Retaining the copyright to your article

Submit your next manuscript at ► [springeropen.com](https://www.springeropen.com)
